PHYSICAL REVIEW C **72**, 041304(R) (2005)

Low momentum shell model effective interactions with all-order core polarizations

Jason D. Holt,[1] Jeremy W. Holt,[1] T. T. S. Kuo,[1] G. E. Brown,[1] and S. K. Bogner[2]
[1]*Department of Physics, State University of New York, Stony Brook, New York 11794, USA*
[2]*Department of Physics, The Ohio State University, Columbus, Ohio 43210, USA*
(Received 5 April 2005; published 31 October 2005)

An all-order summation of core-polarization diagrams using the low-momentum nucleon-nucleon interaction $V_{\mathrm{low}-k}$ is presented. The summation is based on the Kirson-Babu-Brown (KBB) induced interaction approach in which the vertex functions are obtained self-consistently by solving a set of nonlinear coupled equations. It is found that the solution of these equations is simplified using $V_{\mathrm{low}-k}$, which is energy independent, and using the Green's functions in the particle-particle and particle-hole channels. We have applied this approach to the *sd*-shell effective interactions and find that the results we calculated to all orders by using the KBB summation technique are remarkably similar to those of second-order perturbation theory, the average differences being less than 10%.

DOI: 10.1103/PhysRevC.72.041304 PACS number(s): 21.60.Cs, 21.30.−x, 21.10.−k

Since the early works of Bertsch [1] and Kuo and Brown [2], the effect of core polarization (CP) in nuclear physics has received much attention. CP is particularly important in the shell-model effective interactions, where this process provides the long-range internucleon interaction mediated by excitations of the core [3]. In microscopic calculations of effective interactions, CP has played an essential role, as illustrated by the familiar situation in ^{18}O. There the spectrum calculated with the bare G matrix was too compressed compared with experiment, while the inclusion of CP had the desirable effect of both lowering the 0^+ ground state and raising the 4^+ state, leading to a much-improved agreement with experiment [1,2]. As pointed out by Zuker [4], the Kuo-Brown matrix elements, although developed quite some time ago, continue to be a highly useful shell-model effective interaction. It should be noted that the CP diagrams associated with the above interactions were all calculated to second order (in the G matrix) in perturbation theory. However, what are the effects of CP beyond second order, and how can they be calculated? In this communication we address these questions and present an all-order summation of CP diagrams for the *sd*-shell interactions.

There have been a number of important CP studies beyond second order. Third-order CP diagrams, including those with one fold, were studied in detail by Barrett and Kirson [5] for the *sd*-shell effective interactions. Hjorth-Jensen *et al*. [6] have carried out extensive investigations of the third-order CP diagrams for the tin region. A main result of these studies is that the effect of the third-order diagrams is generally comparable with that of the second order; the former cannot be ignored in comparison with the latter. As is well known, high-order CP calculations are difficult to perform, largely because the number of CP diagrams grows rapidly as one goes to higher orders in perturbation theory. The number of diagrams at third order is already quite large, though still manageable. Primarily because of this difficulty, a complete fourth-order calculation has never been carried out. It was soon realized that an order-by-order calculation of CP diagrams beyond third order is not practicable. To fully assess the effects of CP to high order, a nonperturbative method is called for.

The nonperturbative method we use is based on the elegant and rigorous induced interaction approach of Kirson [7] and Babu and Brown [8], hereafter referred to as KBB. Other successful nonperturbative summation methods have also been developed, such as the parquet summation [9] and coupled cluster expansion [10]. In the KBB formalism one obtains the vertex functions by solving a set of self-consistent equations, thereby generating CP diagrams to all orders. Using this approach, Kirson has studied ^{18}O and ^{18}F by using a G-matrix interaction, and Sprung and Jopko [11] have carried out a model study of this approach by using a separable interaction. A main conclusion of both studies is that when CP diagrams are included to all orders the effective interaction is very close to that given by the bare interaction alone. In contrast, Sjöberg [12] applied the Babu-Brown formalism to nuclear matter and found that the inclusion of CP diagrams to all orders has a significant effect on the Fermi liquid parameters in comparison with those given by the bare interaction. These conflicting results for CP studies of finite nuclei and infinite nuclear matter have served as a primary motivation for our present reexamination of the CP effect.

Our application of the KBB formalism to shell-model effective interactions is similar to that of Kirson, but our treatment is different in a number of important regards. As we discuss, the particle-core and hole-core coupling vertices used in the present work include a larger class of diagrams than has been previously studied. We show how the inclusion of these diagrams is facilitated by using the recently developed low-momentum nucleon-nucleon interaction $V_{\mathrm{low}-k}$ [13–19] instead of the previously used G matrix. This is primarily because the G matrix [6,20] depends on both starting energy and the Pauli exclusion operator, while $V_{\mathrm{low}-k}$ depends on neither. It is noted that the S-wave interactions calculated from the Moszkowski-Scott separation method gave essentially the same matrix elements as $V_{\mathrm{low}-k}$ [21]. We now turn our attention to the formal aspects of our approach then discuss

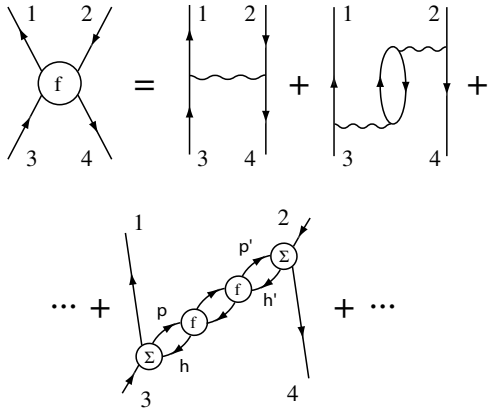

FIG. 1. Self-consistent diagrammatic expansion of the *ph* vertex function f, where Σ is defined in the text.

the application of these methods to the *sd*-shell effective interactions.

The KBB induced interaction approach provides a very appealing way for summing up planar diagrams to all orders. Its fundamental requirement is that the irreducible vertex functions be calculated self-consistently. This means that any CP term contained in a vertex function must be generated self-consistently from the same vertex function. We note that it is this requirement that plays the essential role of generating CP diagrams to all orders. To see this point, it may be convenient to first consider the particle-hole (ph) vertex function f. (We shall consider the particle-particle vertex a little later.) As shown in Fig. 1, f is generated by summation of the driving term V and CP terms, the latter being dependent on f. This then gives the self-consistent equation for f:

$$f = V + \Sigma g_{ph}\Sigma + \Sigma g_{ph} f g_{ph}\Sigma + \Sigma g_{ph} f g_{ph} f g_{ph}\Sigma + \cdots, \tag{1}$$

where g_{ph} is the free ph Green's function and Σ denotes the vertex for particle-core and hole-core coupling. The second-order CP diagram of Fig. 1 is the lowest-order term contained in $\Sigma g_{ph}\Sigma$. We note that, for simplicity, the bra and ket indices have been suppressed in the above equation as well as in the following equations. For example, in Eq. (1) the f on the left-hand side represents $\langle 12^{-1}|f|34^{-1}\rangle$, whereas the fifth and sixth Σs on the right-hand side represent $\langle 1ph^{-1}|\Sigma|3\rangle$ and $\langle 2^{-1}|\Sigma|p'h'^{-1}4^{-1}\rangle$, respectively.

The generation of high-order CP diagrams may be seen easily for the special case $\Sigma = V$. In this case Eq. (1) becomes

$$f = V + V g_{ph} V + V g_{ph} f g_{ph} V + V g_{ph} f g_{ph} f g_{ph} V + \cdots. \tag{2}$$

Since f appears on both sides of this equation, it is clear that an iterative solution for f will yield CP diagrams to all orders, including those with "bubbles inside bubbles," like those shown in diagram (a) of Fig. 2.

For nuclear many-body calculations in general, we also need the particle-particle (pp) vertex function Γ. Like f, Γ is given by a driving term plus CP terms. Furthermore, the diagrammatic representation of Γ is identical to Fig. 1 except

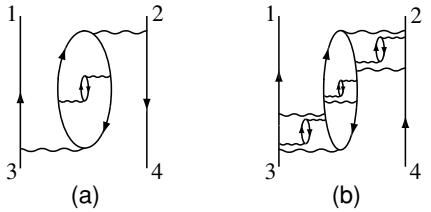

FIG. 2. Higher-order terms contributing to the vertex functions f and Γ, including (a) nested bubbles in bubbles and (b) particle-core and hole-core couplings.

that the hole lines 2 and 4 are replaced with corresponding particle lines. This gives the self-consistent equation for Γ:

$$\Gamma = V + \Sigma g_{ph}\Sigma + \Sigma g_{ph} f g_{ph}\Sigma + \Sigma g_{ph} f g_{ph} f g_{ph}\Sigma + \cdots. \tag{3}$$

To clarify our compact notation, we note that the external lines of the Σ vertices in Γ are different than those shown in Fig. 1. The upper Σ vertex, for example, now represents $\langle 2|\Sigma|ph^{-1}4\rangle$. These different Σ vertices can be related to each other, however, by means of appropriate particle-hole transformations.

Finally, the vertex functions f and Γ are coupled together by means of the coupling vertex Σ. In the present work we choose

$$\begin{aligned} \Sigma &= V + \Sigma_{ph} + \Sigma_{pp}, \\ \Sigma_{ph} &= V g_{ph} V + V g_{ph} f g_{ph} V + V g_{ph} f g_{ph} f g_{ph} V + \cdots, \\ \Sigma_{pp} &= V g_{pp} V + V g_{pp}\Gamma g_{pp} V + V g_{pp}\Gamma g_{pp}\Gamma g_{pp} V + \cdots, \end{aligned} \tag{4}$$

where g_{pp} is the free pp Green's function.

The self-consistent vertex functions f and Γ are determined from Eqs. (1), (3), and (4). These are similar to the equations used by Kirson [7], except that our Σ includes both Σ_{ph} and Σ_{pp}, while the equivalent term in Kirson's calculations includes only Σ_{ph} [7,22]. To see the role of the Σ vertices, let us consider diagram (b) of Fig. 2. Here the lower particle-core vertex, which contains repeated particle-particle interactions, belongs to Σ_{pp}, while the upper one, which contains repeated particle-hole interactions, belongs to Σ_{ph}. It is, of course, necessary to include Σ_{pp} in order to have such CP diagrams in the all-order sum. Our equations are equivalent to those of Kirson when Σ_{pp} is set to zero, and in this case Γ does not enter the calculation of f.

Solving the above equations for f and Γ may seem complicated, but we have found their solution can be simplified significantly through use of the true ph and pp Green's functions:

$$\begin{aligned} G_{ph} &= g_{ph} + g_{ph} f G_{ph}, \\ G_{pp} &= g_{pp} + g_{pp}\Gamma G_{pp}. \end{aligned} \tag{5}$$

When these Green's functions are used to partially sum and regroup our series, the self-consistent Eqs. (1), (3), and (4)

assume a much simpler form

$$f = V + \Sigma G_{ph} \Sigma,$$
$$\Gamma = V + \Sigma G_{ph} \Sigma, \quad (6)$$
$$\Sigma = V + V G_{ph} V + V G_{pp} V.$$

The above simplifications also aid our numerical efforts, and, using the following iterative method, we find that our coupled equations can be solved rather efficiently. For the nth iteration, we start from $f^{(n)}$ and $\Gamma^{(n)}$ to first calculate $G_{ph}^{(n)}$ and $G_{pp}^{(n)}$ followed by $\Sigma^{(n)}$, as seen from Eqs. (5) and (6). We then obtain the vertex functions for the subsequent iteration by taking $f^{(n+1)} = V + \Sigma^{(n)} G_{ph}^{(n)} \Sigma^{(n)}$ and $\Gamma^{(n+1)} = V + \Sigma^{(n)} G_{ph}^{(n)} \Sigma^{(n)}$. The entire iterative process begins from the initial $f^{(0)} = V + V g_{ph} V$ and $\Gamma^{(0)} = V + V g_{ph} V$ and typically converges after just a few iterations.

In the present work, we have included folded diagrams to all orders. As detailed in [23], we use this method to reduce the full-space nuclear many-body problem $H\Psi_n = E_n \Psi_n$ to a model-space problem $H_{\text{eff}} \chi_m = E_m \chi_m$, where $H = H_0 + V$, $H_{\text{eff}} = H_0 + V_{\text{eff}}$, and V denotes the bare NN interaction. The effective interaction V_{eff} is given by the folded-diagram expansion

$$V_{\text{eff}} = \hat{Q} - \hat{Q}' \int \hat{Q} + \hat{Q}' \int \hat{Q} \int \hat{Q} - \cdots. \quad (7)$$

We consider the effective interactions for valence nucleons, and in this case $\hat{Q}$ is the irreducible pp vertex function that we shall calculate by using the KBB equations. In Ref. [7], the effect of higher-order CP diagrams to the nonfolded $\hat{Q}$ term was extensively studied. In the present work, we first calculate $\hat{Q}$ including CP diagrams to all orders. Then we sum the above folded-diagram series for V_{eff} to all orders by using the Lee-Suzuki iteration method as discussed in Ref. [6]. In this way, folded CP diagrams are included to all orders.

For the present calculation we have chosen to use the low-momentum nucleon-nucleon interaction, $V_{\text{low}-k}$. Since the vertex functions f and Γ both depend on the starting energy, there would be off-energy-shell effects present in many CP diagrams if the G-matrix interaction were chosen. This would make the calculation very complicated. $V_{\text{low}-k}$, on the other hand, is energy independent, so no such difficulties are encountered. Because detailed treatments of $V_{\text{low}-k}$ have been given elsewhere [13–19], here we provide only a brief description. We define $V_{\text{low}-k}$ through the T-matrix equivalence $T(p', p, p^2) = T_{\text{low}-k}(p', p, p^2); (p', p) \leqslant \Lambda$, where T is given by the full-space equation $T = V_{NN} + V_{NN} g T$ and $T_{\text{low}-k}$ is given by the model-space (momenta $\leqslant \Lambda$) equation $T_{\text{low}-k} = V_{\text{low}-k} + V_{\text{low}-k} g T_{\text{low}-k}$. Here V_{NN} represents some realistic NN potential and Λ is the decimation momentum beyond which the high-momentum components of V_{NN} are integrated out. $V_{\text{low}-k}$ preserves both the deuteron binding energy and the low-energy scattering phase shifts of V_{NN}. Since empirical nucleon scattering phase shifts are available up to only the pion production threshold ($E_{\text{lab}} \sim 350$ MeV), beyond this momentum the realistic NN potentials cannot be uniquely determined. Accordingly, we choose $\Lambda \approx 2.0$ fm^{-1}, thereby retaining only the information from a given potential that is constrained by experiment. In fact, for this Λ, the $V_{\text{low}-k}$ derived from various NN potentials [24–27] are all nearly identical [17]. Except where noted otherwise, in our calculations we employ the $V_{\text{low}-k}$ derived from the change-dependent (CD) Bonn potential [24].

As an initial study, we carried out a restricted all-order CP calculation for the *sd*-shell effective interactions. In particular, we summed only the TDA diagrams for the Green's functions G_{pp} and G_{ph}, leaving a study of RPA diagrams to a future publication. We used two choices for the shell-model space: One with four shells (10 orbits from $0s_{1/2}$ to $1p_{1/2}$) and the other with five shells (15 orbits from $0s_{1/2}$ to $3s_{1/2}$), both with oscillator constant $\hbar\omega = 14$ MeV. Only core excitations within this space are included. Vary, Sauer, and Wong [28] have pointed out that for CP diagrams one needs to include intermediate states of high excitation energies (up to $\sim 10\hbar\omega$) in order for the second-order CP term to converge. In their work a G matrix derived from the Reid soft-core potential was used, and our use of $V_{\text{low}-k}$ may yield different results as it has greatly reduced high-momentum components. We found that the difference between our five-shell and four-shell calculations was minimal; the results differing by about 2% or less. This finding is supported by recent studies that show desirable convergence properties of $V_{\text{low}-k}$ [29]. We plan to study this convergence problem for $V_{\text{low}-k}$ in the near future.

With these restrictions, we calculated V_{eff} from Eqs. (5)–(7). A large number of angular-momentum recouplings are involved in calculating the CP diagrams. In this regard, we followed closely the diagram rules in [30]. Previous second-order calculations [6,13] included in the $\hat{Q}$ box the first-order pp diagram, the second-order pp and hh ladder diagrams, and the second-order CP diagram. Our all-order calculation includes these same diagrams except the second-order CP diagram is replaced with the all-order CP diagrams from KBB. In Fig. 3 we compare the *sd*-shell V_{eff} matrix elements we

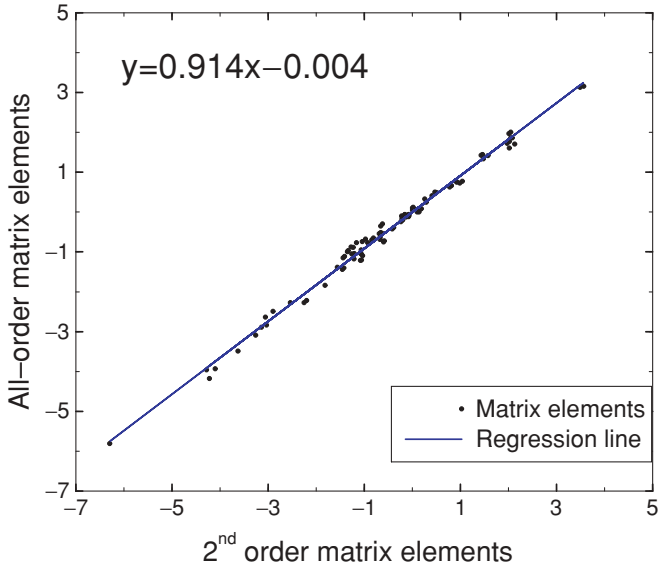

FIG. 3. (Color online) A comparison of the second-order CP matrix elements with those of the all-order KBB calculation.

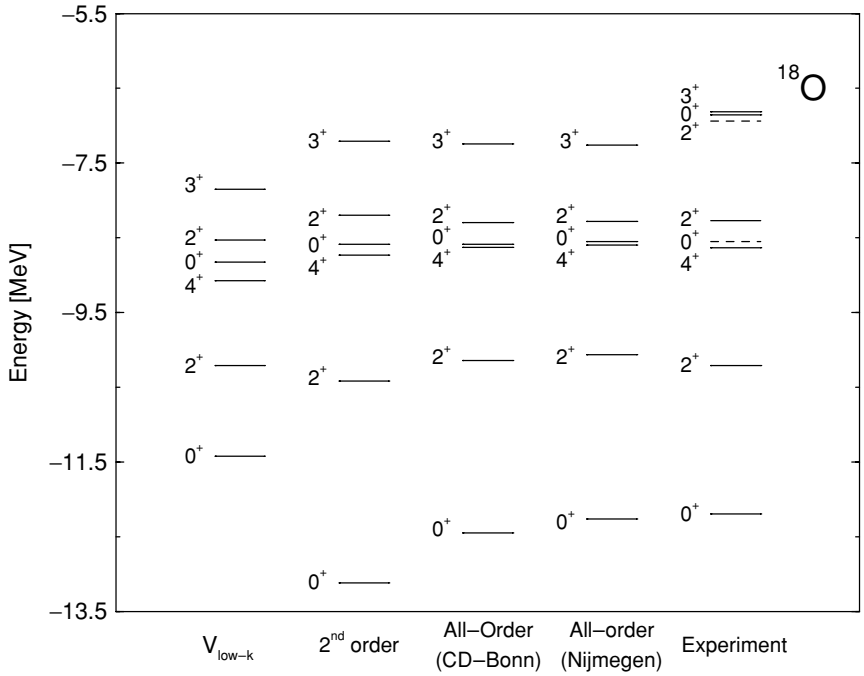

FIG. 4. Spectra for the ^{18}O system calculated to different orders in perturbation theory. Dashed lines for the experimental levels [31] indicate levels with large intruder state mixing [32,33]. All calculations were performed with the experimental single-particle energies of ^{17}O.

calculated from the second-order and all-order $\hat{Q}$ boxes just described, both by using the five-shell space mentioned above. A least-squares fit was applied to the data, and it is apparent that the effect of including CP to all orders in our calculation is a mild suppression of the second-order contributions. This conclusion is further born out in the calculation of the ^{18}O and ^{18}F spectra, the results of which are shown in Figs. 4 and 5. Here we observe a weak suppression of the second-order effects in ^{18}O but a moderate suppression in ^{18}F. In the same figures we also observe that the spectra for different $V_{\text{low}-k}$ derived from the CD Bonn and Nijmegen bare potentials are nearly identical.

In summary, we have presented a method based on the KBB induced interaction formalism for efficiently summing CP diagrams to all orders in perturbation theory. This summation is carried out by way of the KBB self-consistent equations whose solution is significantly simplified by the use of the true *pp* and *ph* Green's functions, and by the use of the energy-independent $V_{\text{low}-k}$. Although our calculation was restricted in several important aspects, we find that our final renormalized interaction

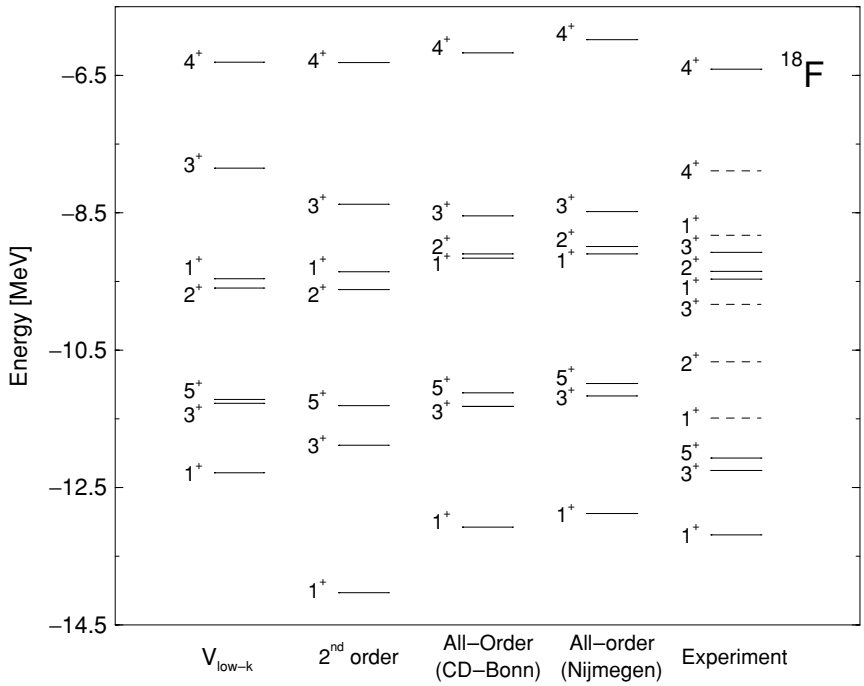

FIG. 5. Spectra for the ^{18}F system calculated to different orders in perturbation theory. See the caption to Fig. 4 for details.

is remarkably close to that of second-order perturbation theory. This is of practical importance and a welcoming result, for it allows one to use the results from a second-order calculation to approximate the contributions resulting from a large class of higher-order diagrams. In the future we intend both to expand our treatment by including additional diagrammatic contributions (RPA) and to generalize our method to study the all-order CP effects for effective operators such as magnetic moments.

We thank M. Kirson for helpful discussions. Partial support from the U.S. Department of Energy under contract DE-FG02-88ER40388 is gratefully acknowledged.

[1] G. F. Bertsch, Nucl. Phys. **74**, 234 (1965).
[2] T. T. S. Kuo and G. E. Brown, Nucl. Phys. **85**, 40 (1966).
[3] G. E. Brown, *Unified Theory of Nuclear Models and Forces* (North-Holland, Amsterdam, 1971).
[4] A. P. Zuker, Phys. Rev. Lett. **90**, 042502 (2003).
[5] B. R. Barrett and M. W. Kirson, Nucl. Phys. **A148**, 145 (1970).
[6] M. Hjorth-Jensen, T. T. S. Kuo, and E. Osnes, Phys. Rep. **261**, 126 (1995), and references therein.
[7] M. W. Kirson, Ann. Phys. (NY) **66**, 624 (1971) ; **68**, 556 (1971); **82**, 345 (1974).
[8] S. Babu and G. E. Brown, Ann. Phys. (NY) **78**, 1 (1973).
[9] A. Jackson, A. Lande, and R. A. Smith, Phys. Rep. **86**, 55 (1982); A. Lande and R. A. Smith, Phys. Rev. A **45**, 913 (1992) .
[10] D. J. Dean and M. Hjorth-Jensen, Phys. Rev. C **69**, 054320 (2004).
[11] D. W. L. Sprung and A. M. Jopko, Can. J. Phys. **50**, 2768 (1972).
[12] O. Sjöberg, Ann. Phys. (NY) **78**, 39 (1973).
[13] S. Bogner, T. T. S. Kuo, L. Coraggio, A. Covello, and N. Itaco, Phys. Rev. C **65**, 051301(R) (2002).
[14] T. T. S. Kuo, S. K. Bogner, and L. Coraggio, Nucl. Phys. **A704**, 107c (2002).
[15] L. Coraggio *et al*., Phys. Rev. C **66**, 021303(R) (2002).
[16] L. Coraggio, A. Covello, A. Gargano, N. Itaco, and T. T. S. Kuo, Phys. Rev. C **66**, 064311 (2002).
[17] S. K. Bogner, T. T. S. Kuo, and A. Schwenk, Phys. Rep. **386**, 1 (2003).
[18] J. D. Holt, T. T. S. Kuo, G. E. Brown, and S. K. Bogner, Nucl. Phys. **A733**, 153 (2004).
[19] J. D. Holt, T. T. S. Kuo, and G. E. Brown, Phys. Rev. C **69**, 034329 (2004).
[20] E. M. Krenciglowa, C. L. Kung, T. T. S. Kuo, and E. Osnes, Ann. Phys. (NY) **101**, 154 (1976).
[21] J. W. Holt and G. E. Brown, nucl-th/0408047.
[22] P. J. Ellis and E. Osnes, Rev. Mod. Phys. **49**, 777 (1977).
[23] T. T. S. Kuo and E. Osnes, in *Lecture Notes in Physics* (Springer-Verlag, New York, 1990), Vol. 364.
[24] R. Machleidt, Phys. Rev. C **63**, 024001 (2001).
[25] R. B. Wiringa, V. G. J. Stoks, and R. Schiavilla, Phys. Rev. C **51**, 38 (1995).
[26] V. G. J. Stoks, R. A. M. Klomp, C. P. F. Terheggen, and J. J. de Swart, Phys. Rev. C **49**, 2950 (1994).
[27] D. R. Entem, R. Machleidt, and H. Witala, Phys. Rev. C **65**, 064005 (2002).
[28] J. P. Vary, P. U. Sauer, and C. W. Wong, Phys. Rev. C **7**, 1776 (1973).
[29] S. K. Bogner, A. Schwenk, R. J. Furnstahl, and A. Nogga, nucl-th/0504043.
[30] T. T. S. Kuo, J. Shurpin, K. C. Tam, E. Osnes, and P. J. Ellis, Ann. Phys. (NY) **132**, 237 (1981).
[31] D. R. Tilley, H. R. Weller, C. M. Cheves, and R. M. Chasteler, Nucl. Phys. **A595**, 1 (1995).
[32] B. H. Wildenthal, Prog. Part. Nucl. Phys. **11**, 5 (1984).
[33] B. A. Brown and B. H. Wildenthal, Annu. Rev. Nucl. Part. Sci. **38**, 29 (1988).